Received: 2 January 2017 | Accepted: 1 June 2017

DOI: 10.1111/ijag.12278

INTERNATIONAL JOURNAL OF
Applied Glass
SCIENCE

ORIGINAL ARTICLE

Full-field measurement of contact-point and crack-tip deformations in soda-lime glass. Part-I: Quasi-static Loading

Balamurugan M. Sundaram | **Hareesh V. Tippur**

Department of Mechanical Engineering, Auburn University, Auburn, Alabama

Correspondence
Hareesh V. Tippur
Email: tippuhv@auburn.edu

Funding information
U.S. Army Research Office, Grant/Award Number: W911NF-16-1-0093, W911NF-15-1-0357 (DURIP)

Abstract

Transparent brittle ceramics such as soda-lime glass pose unique challenges for performing full-field optical measurement of deformations and stresses to characterize fracture and failure behaviors. Low fracture toughness coupled with high stiffness and elastic wave speeds are among the factors responsible for some of these challenges as deformations tend to be small and confined to an extremely small region near the stress concentrators. Need for strong birefringence, elaborate optics, or lack of sufficient measurement sensitivity are some of the factors against legacy techniques such as photoelasticity, optical interferometry, and speckle methods, respectively, to study soda-lime glass. Motivated by these factors, the feasibility of Digital Gradient Sensing (DGS) method to measure crack-tip and contact-induced deformations in soda-lime glass under quasi-static loading is demonstrated. This first of a two parts paper demonstrates the applicability of DGS for the problem under quasi-static loading condition. The optical measurements are used to evaluate the relevant parameters and compare with the analytical solutions. The second part of this study is focused on measuring contact-point and crack-tip deformations during impact-induced stress wave loading.

KEYWORDS

Digital Gradient Sensing, contact stress, fracture mechanics, optical metrology, transparent ceramics

1 | INTRODUCTION

Soda-lime glass is a common engineering material that accounts for over 90% of manufactured glasses. Superior optical transparency, good scratch resistance, high stiffness and hardness, very high compression strength, excellent heat, and chemical resistance are some of the many attractive features that make glass popular for structural applications besides its low cost, recyclability, sustainability, and architectural esthetics. Further, polymer-laminated glasses[1] are found in many other applications, including automotive windshields, windows, etc. Yet, this brittle material suffers from inadequacies such as low fracture toughness presenting the possibility of catastrophic failure during service. In applications such as electronic displays and window panes where stresses due to contact loading or those around pre-existing flaws drastically affect its performance.

Given its low fracture toughness, failure of glass is generally abrupt and catastrophic in the presence of flaws, surface scratches and/or cracks. Performing full-field, noncontact measurement of deformations and stresses to evaluate mechanical properties of glass could prove beneficial for improving it's performance as well as isolating/locating flaws in them which could otherwise be detrimental. For example, the surface flaws generated while handling glass may not be readily visible to the naked eye but they significantly affect the mechanical strength. Additional challenges such as extremely small and highly localized region of intense deformations due to cracks, notches and other stress concentrations pose difficulties to measurement methods. Most reported

works on glasses[2-4] have often relied on postmortem inspection of fracture surfaces and/or crack growth morphologies. As glass is weakly birefringent relative to its strain at failure, it is difficult to obtain sufficient number of fringes to effectively analyze them photoelastically. An attempt in this regard by Voloshin and Burger[5] to analyze the stress field, using the so-called half- fringe photoelasticity is noteworthy. The method of caustics has also been used in the past to study crack-tip and contact stress problems under quasi-static loading conditions.[6,7]

The lack of a suitable, easy to implement, full-field, noncontact optical technique to study glass (and transparent ceramics in general) has been somewhat striking and needs attention. In this context, this work examines the feasibility of a full-field optical technique called Digital Gradient Sensing (DGS)[8] to tackle the stated problem. In DGS, the elasto-optic effects exhibited by transparent soda-lime glass subjected to nonuniform state-of-stress are quantified by evaluating the angular deflections of light rays propagating through the material. The angular deflection measurements represent two orthogonal in-plane stress gradients under plane stress conditions. The presence of stress singularity at an impact point or a crack-tip makes DGS highly effective not only for mechanical field measurements but for locating the stress risers. Authors have previously reported various studies on transparent polymers[9,10] demonstrating the efficacy of DGS. The current work is an attempt to extend it to study extremely brittle material such as soda-lime glass. As noted earlier, the angular deflections produced in glass are extremely small. Hence, the experimental parameters had to be altered to tackle this challenge.

In this work, the working principle of DGS and its extension to higher stiffness material such as soda-lime glass is detailed first. The governing equation and its advantages are detailed next. Two different experiments are reported in this study to demonstrate the feasibility of the DGS for performing accurate and reliable measurements in soda-lime glass under quasi-loading conditions. First, stress concentration due to line-load acting on the edge of a planar sheet is studied. The load histories are evaluated from the DGS measurements and compared with that obtained from a load-cell. Second, deformations near a notch-tip due to the applied loads are studied. Stress intensity factors (SIFs) are evaluated from experiments and examined relative to analytical counterparts. The results are summarized at the end of the report.

2 | DIGITAL GRADIENT SENSING (DGS)

2.1 | Experimental details

A schematic of the experimental setup for transmission-mode DGS technique is shown in Figure 1. In this technique[8], a planar surface spray painted with random speckles, henceforth referred to as "target,"is photographed through a planar transparent sheet being studied. Ordinary white light illumination is used for recording the gray scales on the target. The speckle pattern is first photographed through the specimen in its undeformed state to obtain a reference image. That is, a point P on the target plane (x_0-y_0 plane) is recorded by the camera through point O on the specimen plane ($x-y$ plane). Upon loading, the nonuniform stresses due to the imposed loads change the refractive index of the specimen in the crack-tip vicinity. Additionally, the Poisson effect produces nonuniform thickness changes. A combination of these, commonly referred to as the elasto-optic effect, makes the light rays to deviate from their original path as they propagate in the vicinity of the stress riser such as a crack-tip. The speckle pattern is once again photographed through the specimen in the deformed state. Now, a neighboring point Q on the target plane is recorded by the camera through point O on the specimen plane after deformation. The local deviations of light rays can be quantified by correlating speckle images in the deformed and reference states to find speckle displacements δ_x and δ_y. The angular deflections of light rays ϕ_x and ϕ_y in two orthogonal planes ($x-z$ and $y-z$ planes with the z-axis coinciding with the optical/camera axis of the setup and $x-y$ being the specimen plane coordinates) can be computed if the distance between the specimen plane and the target plane is known. A detailed analysis under paraxial conditions shows that the local angular deflections are related to the gradients of in-plane normal stresses as,

$$\phi_{x;y} = \pm\, C_\sigma B \frac{\partial(\sigma_x + \sigma_y)}{\partial(x;y)} \tag{1}$$

It is important to note that while recording the images, the camera is focused on the "target" (and speckles) through the transparent sheet. Yet, the analysis requires mechanical fields described on the specimen plane, situated at a distance L from the target. That is, a point O(x, y) on the specimen corresponds to a point P(x_0, y_0) on the target plane as shown in the 2D schematic (see, Figure 2). This can be accomplished using a pin-hole camera approximation for which a mapping function between the specimen and the target planes can be deduced. In Figure 2, $\tan\theta = \frac{\delta_s}{L} = \frac{\delta_t}{L+\Delta}$, where δ_s and δ_t are identified on the specimen and target planes, respectively. Hence $\delta_s = (L/(L+\Delta))\delta_t$. (A similar mapping function for the horizontal plane is obvious and should be understood.) Glass being a very brittle, low toughness material, the resulting angular deflections due to applied load are generally very small (a few micro-radians). Hence, Δ needs to be increased significantly to accommodate for this, different from the assumption of $\Delta \ll L$ made by the authors' in

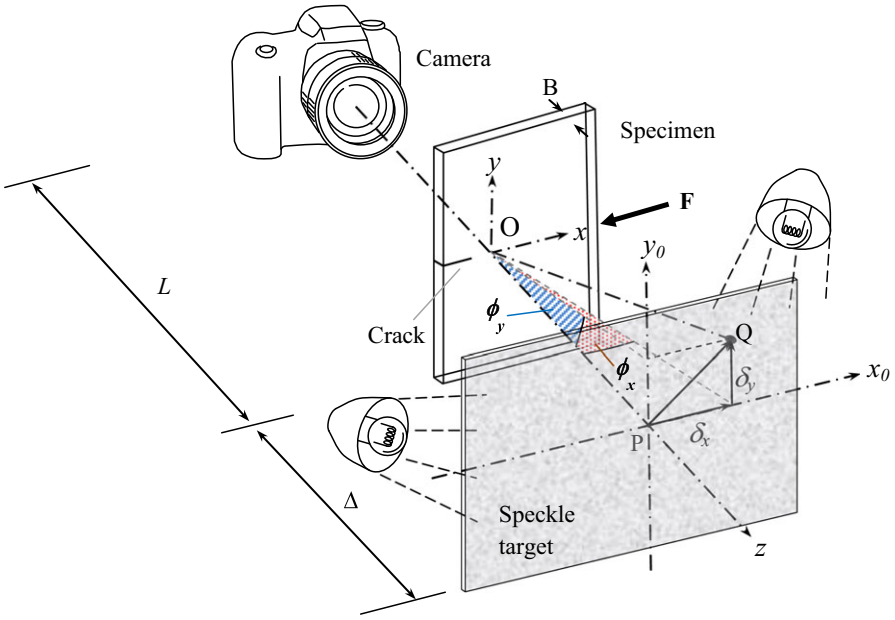

FIGURE 1 The schematic of the experimental setup for transmission-mode Digital Gradient Sensing (DGS) technique to determine stress gradients in transparent sheets [8] [Color figure can be viewed at wileyonlinelibrary.com]

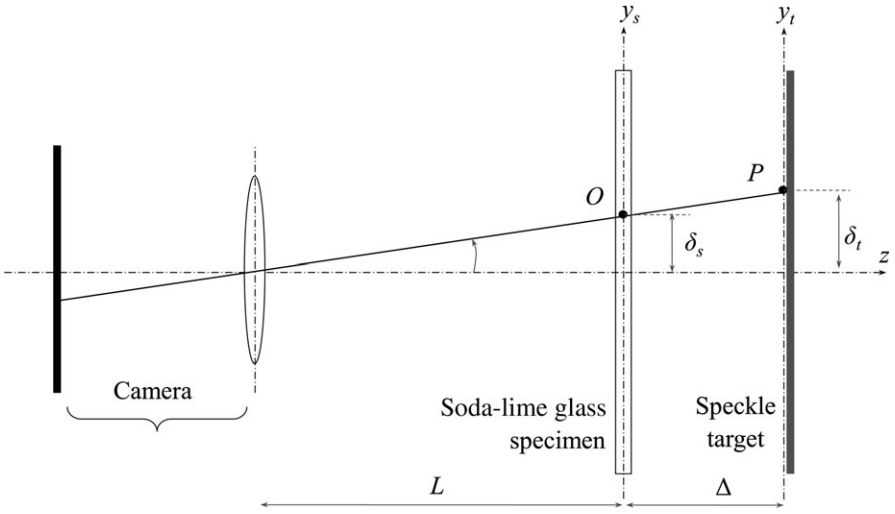

FIGURE 2 2D Schematic for mapping target plane coordinates to the specimen plane coordinates[8]

earlier investigations[9-11] on polymers, and necessitates accounting for the perspective effect during analysis.

2.2 | Advantages of DGS

Transmission DGS is a full-field optical methodology that exploits the technique of 2D digital image correlation (DIC) in conjunction with elasto-optic effect to measure angular deflections of light rays and thus stress gradients. A couple of advantages of the method relevant to this research are (i) the singularity in the measured crack-tip fields facilitates locating the crack-tip more reliably (see[9] for details), and (ii) the ability to easily tune (increase in this case) the measurement sensitivity to deal with the high material stiffness coupled with low toughness of glass that results in extremely small changes in thickness and refractive index due to the prevailing state of stress. That is, it could be effective despite a low elasto-optic coefficient of soda-lime glass (40-50 times lower in magnitude compared to transparent polymers such as PMMA and PC[6,11]), low fracture toughness (~0.8 MPa$\sqrt{m}$ vs 1.1 and 2.3 MPa$\sqrt{m}$ for PMMA and PC) and high crack speeds (~1500 m/s vs ~300 m/s for PMMA and PC). DGS has a few additional benefits that are noteworthy as well. In DGS, the specimen needs no speckle decoration. Instead, a single planar surface ("target") with the desired speckle decoration can be used repeatedly in multiple experiments without introducing variability to the gaging pattern. This further reduces experimental effort in terms of creating multiple specimens with speckle decoration of comparable if not identical characteristics. Another important advantage of DGS is in studying stress concentration problems. Being

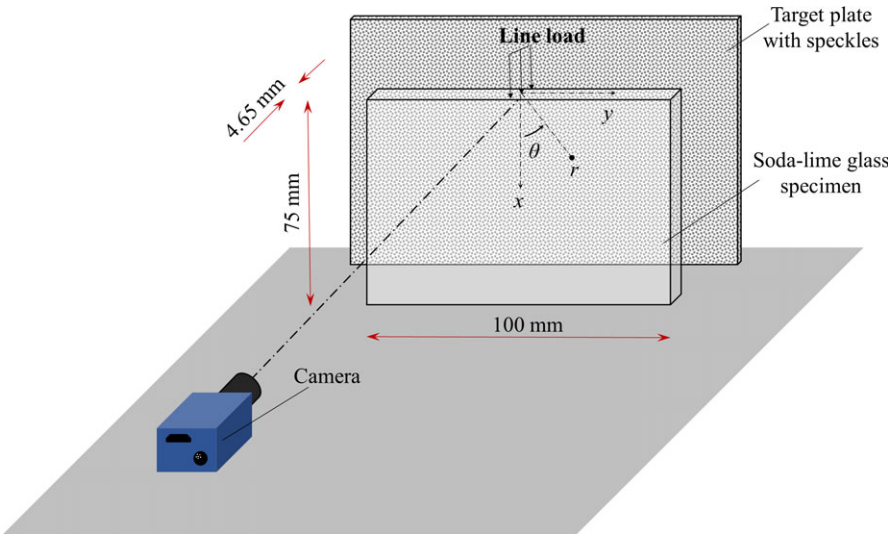

FIGURE 3 Schematic for quasi-static line loading on the edge of a soda-lime glass sheet used in DGS [Color figure can be viewed at wileyonlinelibrary.com]

a stress gradient measurement technique, mechanical fields from DGS, typically visualized as contours of orthogonal angular deflection components, tend to converge to the location of the stress concentration, say, a crack-tip. This greatly assists while identifying the spatial location of the stress singularity in the field-of-view. The availability of orthogonal stress gradients as a rectangular array of data lends itself to an easy implementation of novel 2D integration schemes to estimate stresses accurately via postprocessing of DGS measurements.[12]

3 | LINE-LOAD ON THE EDGE OF A GLASS SHEET

3.1 | Experimental details

A quasi-statically applied line-load on the edge of a large planar glass sheet was studied first. A 100×75 mm^2 rectangular specimen machined from a commercially procured plate glass/soda-lime glass sheet (elastic modulus ~70 GPa, Poisson's ratio 0.22 and C_σ -0.027×10^{-10} m^2/N)[6] of thickness 4.65 mm was used. The schematic of the experimental setup is shown in Figure 3. The specimen was placed on a hardened steel platform and subjected to a line-load, using a cylindrical steel pin (diameter 5 mm attached to an Instron 4465 crosshead) in displacement control mode (crosshead speed ~0.005 mm/s). A target plate painted with random black and white speckles was placed 712 mm away from the specimen mid-plane. A couple of heavy black dots (see, Figure 4) were marked on the speckle plane to relate the image dimensions to the actual target and subsequently the specimen dimensions. A Point Grey Grasshopper3 digital camera with a 18-108 mm focal length zoom lens ($F^{\#}$ 5.6) was used to record speckles through the specimen in the load-point vicinity. The camera was situated at a distance (L) of approximately 445 mm from the specimen plane.

A reference image of the target was recorded through the transparent specimen in the region-of-interest at a small load (<5 N). As the load increased, speckle images were recorded using time-lapse photography (15 frames per minute). Speckle images in the loading point vicinity corresponding to the undeformed and a select deformed (3000 N) state are shown in Figure 4. The recorded images correspond to 63 mm$\times$58 mm region on the target plate which translates to approximately 24 mm$\times$22 mm on the specimen. It shows that due to deformation of the specimen, the speckles appear smeared near the loading point, whereas they seem relatively unaffected far away. Besides this, very little information can be visualized from these speckle images. The digitized speckle images (1184×1100 pixels) recorded at different load levels were correlated with the one corresponding to the reference condition, using image analysis software ARAMIS®. As described previously, an array of in-plane speckle displacements on the target plane (and hence the specimen plane) was evaluated and converted into angular deflections of light rays ϕ_x and ϕ_y. A facet/sub-image size of 25×25 pixels (1 pixel$\approx$53 μm on the target plane) with an overlap of 20 pixels was used in the image analysis for extracting displacement components.

3.2 | Evaluation of load history

The equation for ϕ_x and ϕ_y in terms of the applied load can be described, using the classical Flamant solution,[8]

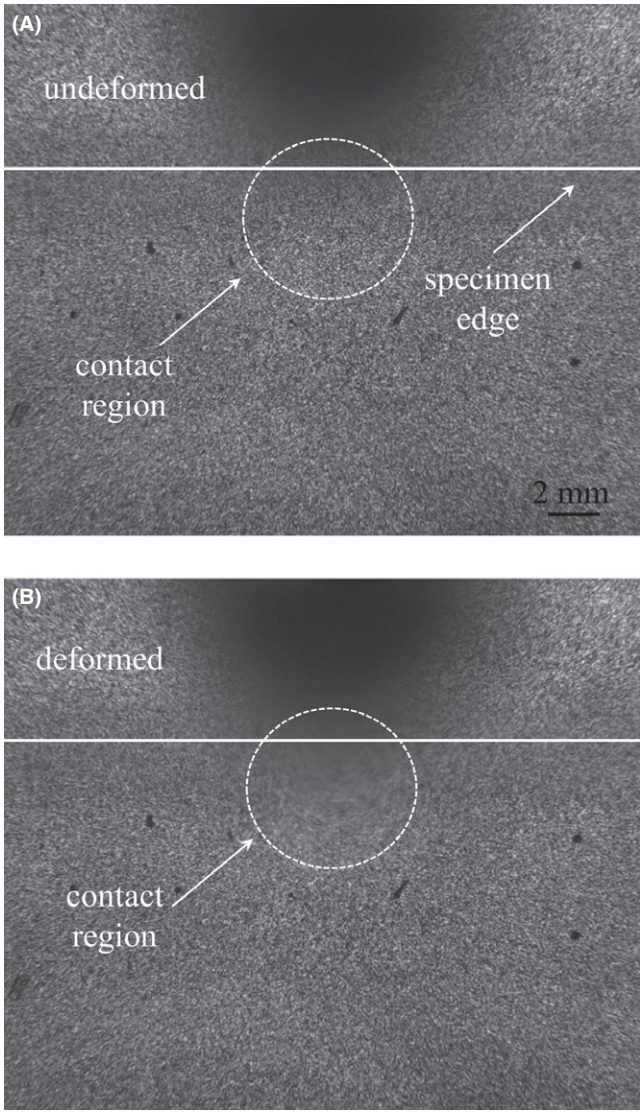

FIGURE 4 Speckle images in the (A) undeformed and (B) deformed states recorded through the soda-lime glass specimen subjected to line-load

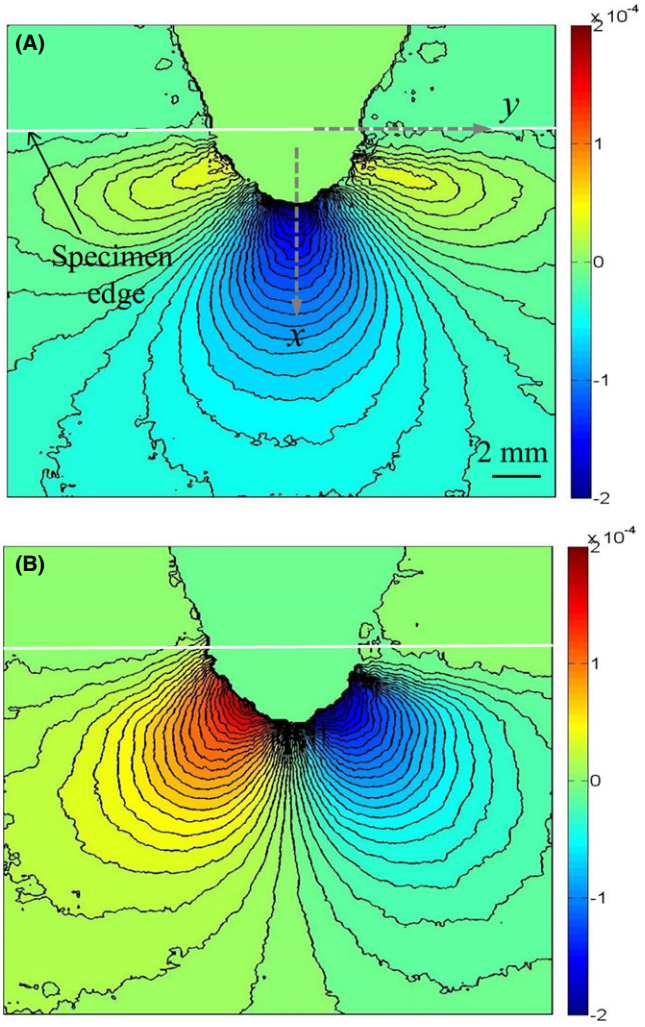

FIGURE 5 Angular deflection contour plots (contour interval=8×10^{-6} rad) proportional to stress gradients of ($\sigma_x+\sigma_y$) in the (A) x- and (B) y-directions for a soda-lime glass specimen under quasi-static line-load on its edge [Color figure can be viewed at wileyonlinelibrary.com]

$$\phi_{x;y} = \pm\, C_\sigma \frac{2F}{\pi}\frac{[\cos(2\theta);\sin(2\theta)]}{r^2} \qquad (2)$$

where C_σ is the elasto-optic constant, F is the applied load and (r, θ) denote polar coordinates defined in Figure 3. The mapping function described in an earlier section was taken into consideration during the analysis. Note that accounting for rigid body motions may be necessary by enforcing boundary conditions of the problem to quantify the contour levels for further analysis. This can be done by forcing symmetry and far-field conditions for this problem as in Ref.[13] The same can also be accomplished by adding constant terms to Equation 2 as,

$$\phi_{x;y} = \pm\, C_\sigma \frac{2F}{\pi}\frac{[\cos(2\theta);\sin(2\theta)]}{r^2} + C_{x;y} \qquad (3)$$

where $C_{x;y}$ denote constants which account for electronic noise and rigid motions if any. In this experiment, F was evaluated using over-deterministic regression analysis of the measured ϕ_x. Alternatively, ϕ_y can also be used to evaluate F. Discrete angular deflection values around the loading point in the region $1\leq r/B\leq 2$ along with an angular extent of $-80°\leq\theta\leq-50°$, $-40°\leq\theta\leq40°$ and $50°\leq\theta\leq80°$ were used in the regression analysis. This ensured avoiding the region of dominant stress triaxiality along the free edges and regions adjacent to zones where angular deflections are nearly zero. This also helped to deal with the lack

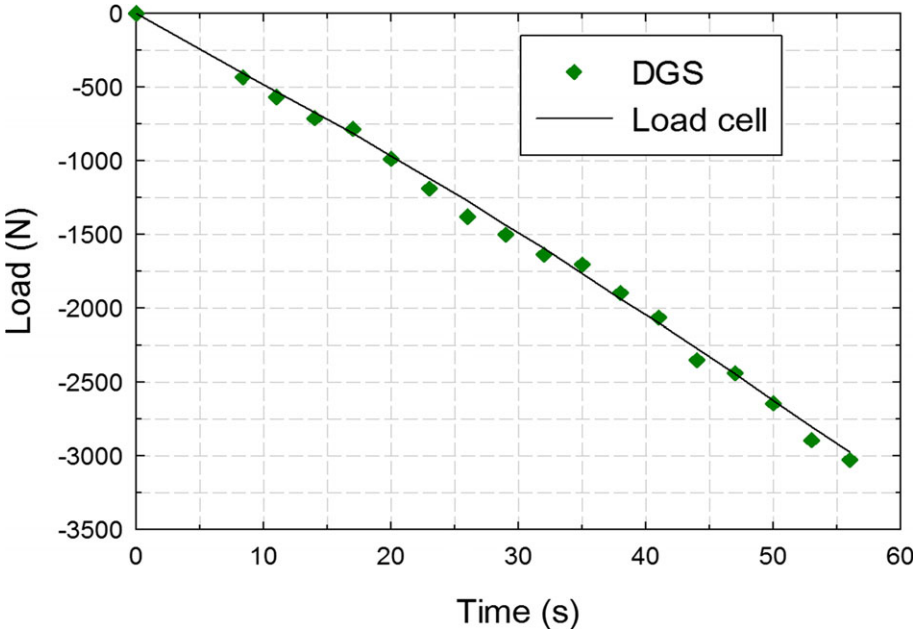

FIGURE 6 Load history obtained from (A) DGS data and (B) load-cell of the testing machine [Color figure can be viewed at wileyonlinelibrary.com]

of data in the close vicinity of the loading point due to finite (limited) numerical aperture of the camera.

3.3 | Experimental results

The measured DGS contours (on the specimen plane) of angular deflections ϕ_x and ϕ_y for a select load of 3000 N are shown in Figure 5. It should be noted that the contours near the free edge of the specimen show unavoidable edge effects. Using Equation 3, the load was extracted at each time step to obtain the load history. By matching the time stamp on the recorded image with the data from the load-cell, another set of load history was obtained. Both the load histories are plotted in Figure 6 and the two are in good agreement with each other.

4 | CRACK-TIP DEFORMATIONS

4.1 | Experimental details

Quasi-static crack-tip deformations were measured next. A soda-lime glass sheet of 4.65 mm thickness was cut to obtain 130 mm×50 mm SENB specimens. A 10 mm long notch was machined into it, using a band saw of 2 mm thickness. The initial notch was intentionally kept wide to avoid premature specimen failure at lower load. The specimen was placed on two anvils (120 mm apart) symmetrically relative to the notch cut along the bottom edge and the loading pin pressing down on the top edge. A symmetric 3-point-bend test was performed on this specimen, using Instron 4465 testing machine in displacement

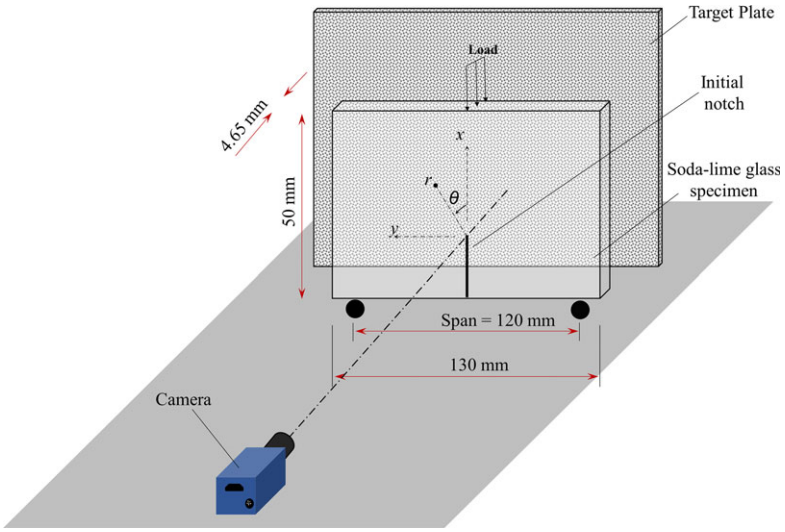

FIGURE 7 Loading configuration for quasi-static 3-point bending of an edge notched soda-lime glass plate [Color figure can be viewed at wileyonlinelibrary.com]

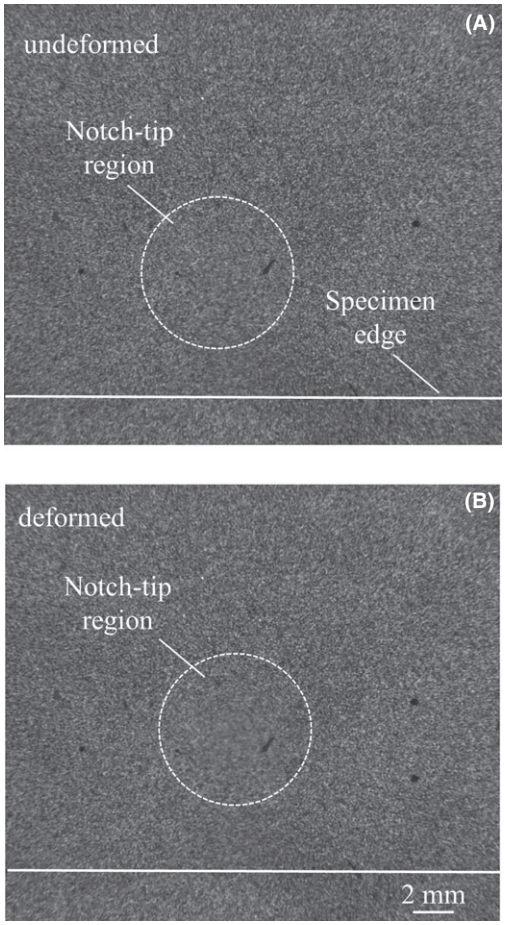

FIGURE 8 Speckle images in the (A) undeformed and (B) deformed states near the initial notch-tip recorded by the camera through the soda-lime glass specimen. (The notch is not in focus)

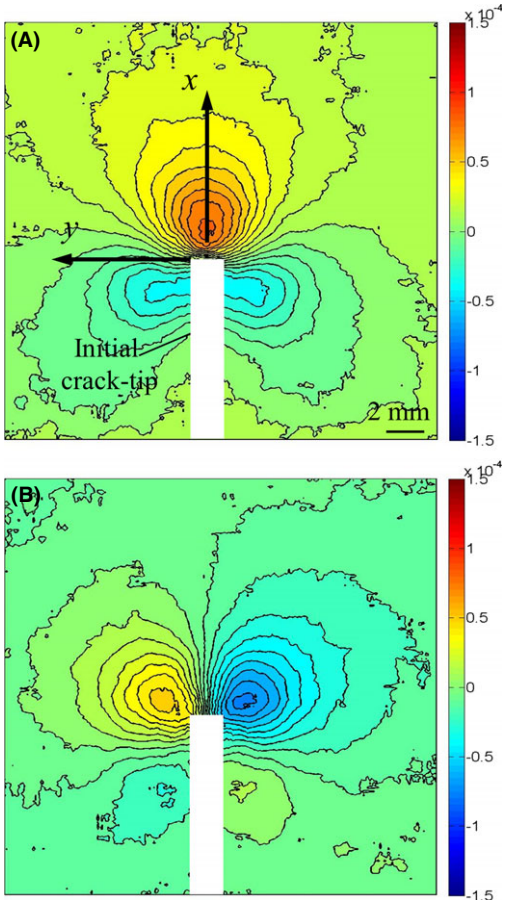

FIGURE 9 Angular deflection contour plots (contour interval=8×10^{-6} rad) proportional to stress gradients of ($\sigma_x+\sigma_y$) in the (A) *x*- and (B) *y*-directions near the notch-tip for a soda-lime glass specimen under quasi-static 3-point bending load [Color figure can be viewed at wileyonlinelibrary.com]

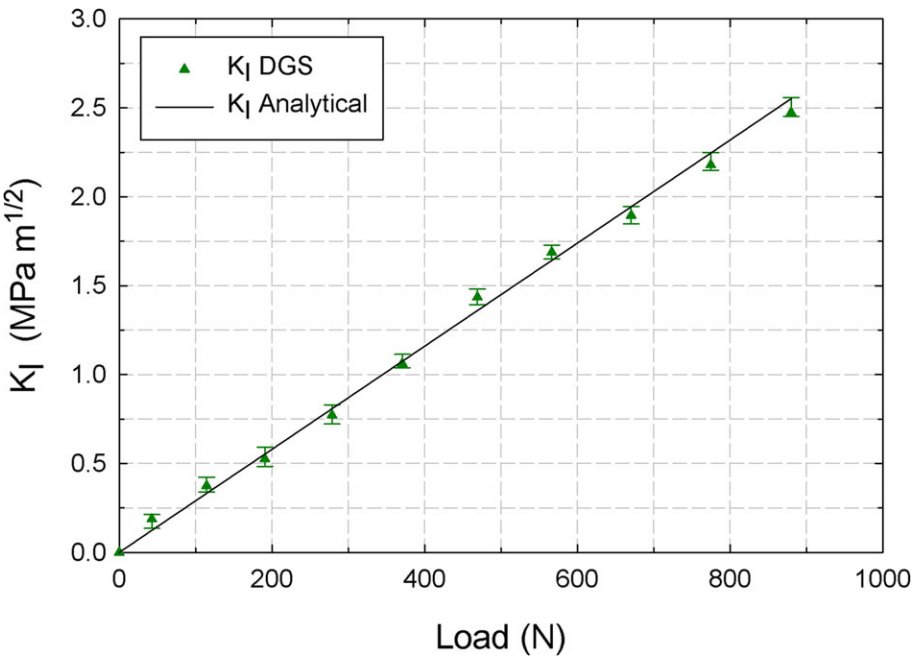

FIGURE 10 Comparison of mode-I stress intensity factors from DGS data and the analytical expression (Equation 6) [Color figure can be viewed at wileyonlinelibrary.com]

control mode (crosshead speed of ~0.005 mm/s). The schematic of the experimental setup used is shown in Figure 7.

The speckled target plate was placed behind the specimen at a distance of Δ ~712 mm from the specimen mid-plane. A Point Grey Grasshopper3 digital camera (spatial resolution of 1184×1100 pixels and 10-bit gray scale resolution) fitted with a macro zoom lens of 18-108 mm focal length ($F^{\#}$ 5.6) was used to record speckles on the target plate as in the previous experiment. The camera was placed in front of the specimen at a distance (L) of ~445 mm with the camera focused on the target plate through the specimen. Two CFL lamps were used to illuminate the target plate uniformly.

A reference speckle image of the target plate was recorded through the crack-tip vicinity at no-load (load<5 N) condition. As the load was increased gradually, the perturbed images of the speckles on the target plate were recorded, using time-lapse photography at 15 frames per minute. Two representative images, one in the reference state and the other in the deformed state, are shown in Figure 8. The recorded images correspond to 63 mm×58 mm region on the target plate which translates to approximately 24 mm×22 mm on the specimen. Using a pair of reference dots (see, Figure 8) marked on the target plate, the dimensions on the image in terms of pixels were related back to target plate dimensions (1 pixel= approx. 53 μm on the target plane) and then to specimen dimensions (1 pixel=approx. 21 μm on the specimen plane). Sufficient care was also exercised to obtain a near Gaussian distribution of gray scales for each image in the mid-range of the gray scale by positioning the lamps appropriately. When looked carefully, the speckles appear slightly smeared in Figure 8B around the crack-tip whereas they seem largely unaffected away from it. The images were again correlated, using ARAMIS® software (GoM GmbH, Braunschweig, Germany). A facet/sub-image size of 25×25 pixels with an overlap of 20 pixels (ie, step size of 5 pixels) was used during speckle correlation. The resulting data matrix was exported to MATLAB for post-processing, including the evaluation of orthogonal angular deflections in the region of interest.

4.2 | Evaluation of stress intensity factor (SIF)

Williams' asymptotic stress fields for angular deflections near a statically loaded mode-I crack-tip become,[9,14]

$$\phi_x = C_\sigma B \frac{\partial(\sigma_x + \sigma_y)}{\partial x} = C_\sigma B \sum_{N=1}^{\infty} A_N \left(\frac{N}{2} - 1\right) r^{\left(\frac{N}{2}-2\right)} \cos\left(\left(\frac{N}{2} - 2\right)\theta\right) \quad (4)$$

$$\phi_y = -C_\sigma B \frac{\partial(\sigma_x + \sigma_y)}{\partial y} = -C_\sigma B \sum_{N=1}^{\infty} A_N \left(\frac{N}{2} - 1\right) r^{\left(\frac{N}{2}-2\right)} \sin\left(\left(\frac{N}{2} - 2\right)\theta\right) \quad (5)$$

where (r,θ) denote the crack-tip polar coordinates, $A_1 = K_I\sqrt{2/\pi}$ with K_I being the mode-I stress intensity factor. (It should be noted that the dominant or the leading term of the crack-tip stress fields for $(\sigma_x + \sigma_y)$ remain unaffected in the classical Creager's solution[15] that takes into account the finite root radius of a notch.) In this experiment, the SIFs were evaluated using Equation 4 by employing an over-deterministic regression analysis of the measured data and N=4. Discrete angular deflection values around the crack-tip in the region $0.5 \le r/B \le 1.5$ along with the angular extent of $-150° \le \theta \le +150°$, was used in the regression analysis. This ensured that the data used was sufficiently close to the crack-tip yet outside the region of significant stress triaxiality. This also indirectly helped to minimize the error while locating the crack-tip due to potential edge effects during image correlation. It should be noted that the mapping function, described in an earlier section, was accounted for during the analysis. Error bars were obtained as a result of uncertainty in locating the crack-tip and by using various subsets of the region described above.

The mode-I SIFs can also be evaluated from the load history obtained from the load-cell and the sample geometry as,[9]

$$K_I = \frac{FS}{Bw^{3/2}} \frac{3(\xi)^{1/2}\left[1.99 - \xi(1-\xi)\left\{2.15 - 3.93(\xi) + 2.7(\xi)^2\right\}\right]}{2(1+2\xi)(1-\xi)^{3/2}}, \xi = \frac{a}{w} \quad (6)$$

where F is the applied load, S is the span, B is the thickness of the specimen, w is the width of the specimen and a is the initial crack length.

4.3 | Experimental results

The angular deflection contours on the specimen plane in two in-plane orthogonal directions at a load of 880 N are shown in Figure 9. A heavy white line is overlaid on the

resulting contours to represent the notch. The mode-I SIFs obtained from the regression analysis of measured data at different imposed load levels is plotted in Figure 10 along with that obtained from the load-cell. Evidently, there is a good agreement between the two.

5 | CONCLUSIONS

The transmission-mode Digital Gradient Sensing (DGS) method has been extended in this work to visualize and quantify orthogonal stress gradient fields in soda-lime glass under quasi-static loading conditions. Typical challenges of studying failure of high stiffness and low toughness transparent ceramics have been overcome by using this full-field speckle-based optical method. The feasibility of DGS to map stress gradient fields due to quasi-statically applied line-load on the edge of a uniformly supported plate and on a symmetrically bent beam with a single edge notch is demonstrated. The full-field measurements have been analyzed to extract the applied load and mode-I stress intensity factor, respectively, in these configurations with good accuracy. Thus, demonstrating the accuracy and robustness of the measurement technique and the methodology of analysis for soda-lime glass.

ACKNOWLEDGMENTS

The support of the U.S. Army Research Office for this research through grants W911NF-16-1-0093 and W911NF-15-1-0357 (DURIP) are gratefully acknowledged.

REFERENCES

1. Patel PJ, Gilde GA, Dehmer PG, McCauley JW. Transparent armour. *AMPTIAC Newslett*. 2000;4. no. 3, Fall 2000.
2. Conrad H, Keshavan MK, Sargent GA. Hertzian fracture of Pyrex glass under quasi-static loading conditions. *J Mater Sci*. 1979;14:1473-1494.
3. Nielsen JH, Olesen JF, Stang H. The fracture process of tempered soda-lime-silica glass. *Exp Mech*. 2009;49(6):855-870.
4. Ayatollahi MR, Aliha MRM. Mixed mode fracture in soda lime glass analyzed by using generalized MTS criterion. *Int J Solids Struct*. 2009;46(2):311-321.
5. Voloshin AS, Burger CP. Half-fringe photoelasticity: a new approach to whole-field stress analysis. *Exp Mech*. 1983;23:304-313.
6. Sih GC. *Experimental Evaluation of Stress Concentration and Stress Intensity Factor*. Boston: Martinus Nijhoff publishers; 1981.
7. Zehnder AT, Rosakis AJ. A note on the measurement of K and J under small-scale yielding conditions using the method of caustics. *Int J Fract*. 1986;30:R43-R48.
8. Periasamy C, Tippur HV. Measurement of orthogonal stress gradients due to impact load on a transparent sheet using digital gradient sensing method. *Exp Mech*. 2013;53:97-111.
9. Sundaram BM, Tippur HV. Dynamic crack growth normal to an interface in bi-layered materials: an experimental study using digital gradient sensing technique. *Exp Mech*. 2016;56:37-57.
10. Sundaram BM, Tippur HV. Dynamics of crack penetration vs. branching at a weak interface: an experimental study. *J Mech Phys Solids*. 2016;96:312-332.
11. Sundaram BM, Tippur HV. Dynamic mixed-mode fracture behaviors of PMMA and polycarbonate. *Eng Fract Mech*. 2017;176:186-212.
12. Miao C, Sundaram BM, Huang L, Tippur HV. Surface profile and stress field evaluation using digital gradient sensing method. *Meas Sci Technol*. 2016;27:095203. no. 9, (16 pp).
13. Periasamy C, Tippur HV. Full-feild digital gradient sensing method for evaluating stress gradients in transparent solids. *Appl Opt*. 2012;51:2088-2097.
14. Williams ML. On the stress distribution at the base of a stationary crack. *J Appl Mech*. 1959;24:109-114.
15. Creager M, Paris PC. Elastic field equations for blunt cracks with reference to stress corrosion cracking. *Int J FractMech*. 1967;3:247-252.

How to cite this article: Sundaram BM, Tippur HV. Full-field measurement of contact-point and crack-tip deformations in soda-lime glass. Part-I: Quasi-static Loading. *Int J Appl Glass Sci*. 2018;9:114-122. https://doi.org/10.1111/ijag.12278